

5-2017

Blood-Brain Barrier-on-a-chip Systems Based on 3D Printing

Cade I. Harding

University of Arkansas, Fayetteville

Follow this and additional works at: <http://scholarworks.uark.edu/meeguht>

 Part of the [Electro-Mechanical Systems Commons](#), and the [Other Biomedical Engineering and Bioengineering Commons](#)

Recommended Citation

Harding, Cade I., "Blood-Brain Barrier-on-a-chip Systems Based on 3D Printing" (2017). *Mechanical Engineering Undergraduate Honors Theses*. 61.

<http://scholarworks.uark.edu/meeguht/61>

This Thesis is brought to you for free and open access by the Mechanical Engineering at ScholarWorks@UARK. It has been accepted for inclusion in Mechanical Engineering Undergraduate Honors Theses by an authorized administrator of ScholarWorks@UARK. For more information, please contact scholar@uark.edu, ccmiddle@uark.edu.

**BLOOD-BRAIN BARRIER-ON-A-CHIP SYSTEMS BASED ON 3D
PRINTING**

BLOOD-BRAIN BARRIER-ON-A-CHIP SYSTEMS BASED ON 3D PRINTING

An Undergraduate Honors College Thesis

in the

Department of Mechanical Engineering

College of Engineering

University of Arkansas

Fayetteville, AR

By

Cade Ingram Harding

April 28, 2017

ACKNOWLEDGEMENTS

I would like to thank Dr. Tung for all the support and guidance throughout my research. Thank you for welcoming me to your research group and providing me with all necessary tools and equipment. Thank you for always answering my repetitive questions, I have learned so much through this process. I would also like to thank the other students working under Dr. Tung, Bo Ma, Zeina Salman, and Kayla Bartnicke, for the training and help with any new experimental technique I was unfamiliar with. Finally, I would like to thank Dr. Huang and Dr. Kim for taking the time to serve on my thesis committee and provide feedback.

I would like to thank the University of Arkansas Honors College for the research grant I received to fund this thesis. I have learned valuable lessons outside of the classroom and gained meaningful lab experience. I am incredibly grateful to have been a part of the Honors College because it has allowed me to gain a broad range of skills and knowledge through research.

Table of Contents

1	ABSTRACT.....	1
2	INTRODUCTION	2
2.1	Research Problem	2
3	BACKGROUND	3
3.1	BBB Environment	4
3.2	Current Research	5
3.3	Prior Work.....	7
4	DESIGN, SIMULATION, AND FABRICATION.....	8
4.1	COMSOL Scaling Tests.....	9
4.2	COMSOL Shear Stress	12
4.3	3D Prints.....	16
5	RESULTS/DISCUSSION	17
5.1	Micropump Test Setup	17
5.2	Micropump Results.....	19
5.2.1	Test Pump 1	19
5.2.2	Test Pump 2	21
5.2.3	Test Pump 3	23
5.2.4	Test Pumps 4 & 5.....	27
6	CONCLUSIONS	30
7	FUTURE WORK.....	30
8	REFERENCES	32
9	APPENDICES	33
9.1	Appendix A – COMSOL Parameters and Results.....	33
9.2	Appendix B – 3D printed models	34

LIST OF FIGURES AND TABLES

Figure 3.1.	Constitution of blood vessels inside the brain [7].....	4
Figure 3.2.	Pneumatically actuated diaphragm for micropump with flow indicated by arrows. (a) Diaphragms in initial position. (b) Small diaphragm deflected causing bi-directional flow. (c) Both diaphragms deflected with backflow prevented by check valve diaphragm. [11].....	8
Figure 4.1.	BBB velocity simulation results.....	12
Table 4.1.	Velocity measurements with theoretical calculations and COMSOL.....	12
Figure 4.2.	(Left) Shear rate across top face of channel; (Right) Shear rate at inlet of channel	13
Figure 4.3.	Wall shear stress at each simulated flow rate	14
Figure 4.4.	Shear rate of 2 mm by 0.5 mm channel at 2502 $\mu\text{L}/\text{min}$	16
Figure 4.5.	“3D model of 3D printed micro-pump. The orange lines indicate the location of the air inlet, and air-chamber aligned to the diaphragms” [11].....	17
Figure 5.1.	(1) Section of tubing used to measure flow rate with ruler; (2) Inlet tubing for compressed gas; (3) Pipette tip for fluid inlet; (4) Taped and secured micropump device – in white.	18
Figure 5.2.	Test Pump 1 top view of cross section, with dimensions	20
Figure 5.3.	Isometric view of Test Pump 1.....	20
Figure 5.4.	Test Pump 2 top view of cross section, with dimensions	21
Figure 5.5.	Isometric view of Test Pump 2.....	22
Figure 5.6.	Test Pump 2 flow rate results	23
Figure 5.6.	Test Pump 3 results at 20 psi	24
Figure 5.7.	Test Pump 3 results at 30 psi	25
Figure 5.8.	Test Pump 3 results at 40 psi	26
Figure 5.9.	Applied shear stress on microchannel walls at each pump actuation pressure	27
Figure 5.10.	Test Pump 4 top view of cross section, with dimensions	27
Figure 5.11.	Isometric view of Test Pump 4.....	27
Figure 5.12.	Test Pump 5 top view of cross section	28
Figure 5.13.	Isometric view of Test Pump 5.....	29
Table A.1.	COMSOL Testing parameters and results (Inlet flow rate OR pressure was required for the simulation).....	33
Figure A.2.	Test Pump 1 (cut in half to investigate problems)	34
Figure A.3.	Test Pump 1 view of cut microchannel	34

Figure A.4.	Test Pump 1 print of cross section	34
Figure A.5.	Test Pump 2 (cut in half to investigate problems)	35
Figure A.6.	Test Pump 2 cross section after cut.....	35
Figure A.7.	Test Pump 3 (working micropump).....	35
Figure A.8.	Test Pump 4	35
Figure A.9.	Test Pump 4 horizontal input.....	36
Figure A.10.	Test Pump 5	36
Figure A.11.	Test Pump 5 with horizontal inlet.....	36

LIST OF EQUATIONS AND SYMBOLS

Eq. 1: $v = \frac{\mu}{\rho}$9

v = Kinematic viscosity (m^2/s)

μ = Dynamic viscosity ($Pa*s$)

ρ = Density (kg/m^3)

Eq. 2: $A_{BBB} = \frac{\pi D^2}{4}$9

A = Area (m^2)

D = Diameter (m)

Eq. 3: $D_H = \frac{2wh}{w+h}$10

D_H = Hydraulic Diameter (m)

w = Width (m)

h = Height (m)

Eq. 4: $A_{rectangle} = wh$10

Eq. 5: $Q = V * A$10

Eq. 6: $Re = \frac{u*L}{v}$10

Re = Reynolds number

L = Characteristic Length (m)

Eq. 7: $Re = \frac{Q D_H}{\mu A}$10

Q = Flow rate (m^3/s)

A = Cross sectional area (m^2)

Eq. 8: $\tau_{BBB} = \frac{4*\mu*Q}{\pi r^3}$10

τ = Shear Stress (Pa)

r = Radius (m)

Eq. 9: $\tau_{rectangle} = \frac{6*\mu*Q}{w*h^2} \left(1 + \frac{h}{w}\right) * f * \left(\frac{h}{w}\right)$10

f = Function variable defined in Reference 8 (not used)

Eq. 10: $\tau_{rectangle} = \frac{6*\mu*Q}{w*h^2}$11

Eq. 11: $\tau = \dot{\gamma} * \mu$13

$\dot{\gamma}$ = Shear rate (1/s)

Eq. 12: $V = \frac{\Delta x}{\Delta t}$18

V = Velocity (m/s)

Δx = Displacement (m)

Δt = Change in time (s)

Eq. 13: $Q = V * A$18

1 ABSTRACT

This research focused on the design and testing of a blood-brain barrier (BBB)-on-a-chip microfluidic device produced using 3D printing. First, COMSOL simulations were used to define dimensions of the microchannel that would most accurately replicate the flow environment imposed on the blood-brain barrier, the wall shear stress being the most important characteristic. In using COMSOL, water was used as the simulated fluid and also the testing fluid in the fabricated devices. Therefore, the microsystem is designed to produce the BBB environment using water instead of blood. The numerical simulation parameters were based on theoretical calculations performed to scale up the dimensions of the brain capillary with the BBB to the dimensions of a microchannel that is possible to 3D print. The COMSOL simulation results show that a rectangular channel with a height of 2 mm and width of 0.5 mm will be under a wall shear stress of approximately 0.43 Pa at 2500 $\mu\text{L}/\text{min}$, 0.75 Pa at 4000 $\mu\text{L}/\text{min}$, and 1.99 Pa at 9000 $\mu\text{L}/\text{min}$.

A micropump designed and tested by Carlton McMullen is used as the standard for new models, which are fabricated using a MakerBot Replicator 2 3D printer [11]. Its pumping capabilities were tested to determine if it could produce the flow rates found in the numerical simulations. The pump was tested at actuation pressures of 20 psi, 30 psi, and 40 psi, while the actuation frequency was held constant at 10 Hz. The average flow rate was 2810 $\mu\text{L}/\text{min}$ at 20 psi, 3420 $\mu\text{L}/\text{min}$ at 30 psi, and 5325 $\mu\text{L}/\text{min}$ at 40 psi. These results indicate that the current micropump could cause a wall shear stress up to 0.87 Pa in the microchannel where the BBB is replicated and studied. This value is within the range of *in vivo* shear stress values, validating this method of using water to recreate the environment. With these flow rate results, the micropump design is capable of producing flow rates required for *in vivo* shear stress values. This research defines 3D printable microchannel dimensions that allow these shear stress values based on attainable flow rates from this micropump.

2 INTRODUCTION

Serious diseases that accompany old-age are becoming more prevalent as life expectancy increases. Many of these diseases, like Alzheimer's and Parkinson's disease, involve the central nervous system. Many medications that treat these diseases must pass through the blood-brain barrier (BBB). Research in new medications has not had much success due to inadequate testing procedures because of the complexity of the BBB. The blood-brain barrier is a permeable membrane that is highly selective and separates the blood from brain tissue. Because of the low permeability, many large molecules and drugs are unable to pass through the membrane [1]. The low permeability of this unique membrane, however, is difficult to produce and simulate. Endothelial cells line the brain capillaries and are supported by astrocyte and pericyte cells, which help create tight junctions to reduce the permeability and keep molecules in the bloodstream and out of the brain. Without including all types of cells, *in vitro* models of the BBB are often unrealistic because the permeability depends on the interactions between all three types of cells. To accurately simulate the BBB and the permeability towards new medications, all three types of cells, endothelial, pericytes, and astrocytes, must be incorporated into the system [2].

Microfluidic devices are becoming a popular source of combining components of *in vivo* and *in vitro* systems. These "Organ-on-a-chip" devices have the capability of introducing live tissue into the device while adjusting the device's environmental parameters, like other *in vitro* systems [13]. As stated previously, the BBB's behavior is caused by many of the surrounding cells. Using organ-on-a-chip technology, all required cells involving the BBB can be grown in the device to increase the similarity to the *in vivo* environment.

2.1 Research Problem

The purpose of this thesis is to build on previous work in microfluidic system components to create a device capable of accurately simulating the environment surrounding the BBB. The

microfluidic device will be used to create conditions similar to those in the brain capillaries, focusing mainly on the shear stress caused by blood flow. Water is used for the device as numerical simulations can be used to predict the shear stress caused by flow of water since it is a Newtonian fluid. Based on an *in vivo* shear stress range, a microchannel will be designed and fabricated using 3D printing that can also be exposed to this shear stress range using water instead of blood. To reach these shear stress values, the flow rate must be optimized with the microchannel dimensions. This research serves to define these parameters with water to supply a device capable of creating the BBB environment that can later be modified for non-Newtonian fluids, like the blood in the capillaries.

3 BACKGROUND

A microfluidic device utilizes research in the field of micro-electro mechanical systems (MEMS). Many microfluidic devices are designed as Lab-on-a-chip or Organ-on-a-chip systems, which means they are used to perform simple laboratory functions at a small scale [3]. These lab functions can include sample preparation, media or liquid transfer through pumps and mixers, and sensing or detection. An example of these functions is two micropumps being used to transport different solutions to a connected mixing reservoir. The solutions can be mixed using a micromixer [4,5]. There are numerous other applications of lab-on-a-chip devices.

Microfluidic devices used for these functions can provide a faster and inexpensive way to complete lab tests. Cost is significantly reduced because at the microscale very small amounts of testing reagents are required. Most current MEMS devices are fabricated with polydimethylsiloxane (PDMS) using various techniques. These techniques can take days of preparation and work to produce molds and masks for one product. This paper focuses on a different option, 3D printing or additive manufacturing, to fabricate each device to save time and

reduce cost. By 3D printing each device, the fabrication method is simplified to designing with a CAD software and allowing a machine to complete the fabrication. 3D printers greatly increase the repeatability of the fabrication process and allow easy design changes without changing any tools [4].

3.1 BBB Environment

As previously stated, the conditions surrounding the BBB must be considered and implemented to accurately simulate the environment. First, the structure of the membrane and surrounding cells play an important role in the permeability. Astrocytes and pericytes work together to form tight junctions around the endothelial cells to communicate with other surrounding to proteins to prevent molecules from passing through the cells. Without the astrocytes and pericytes, these junctions are not formed [2,6]. The image below depicts the BBB structure with these surrounding cells.

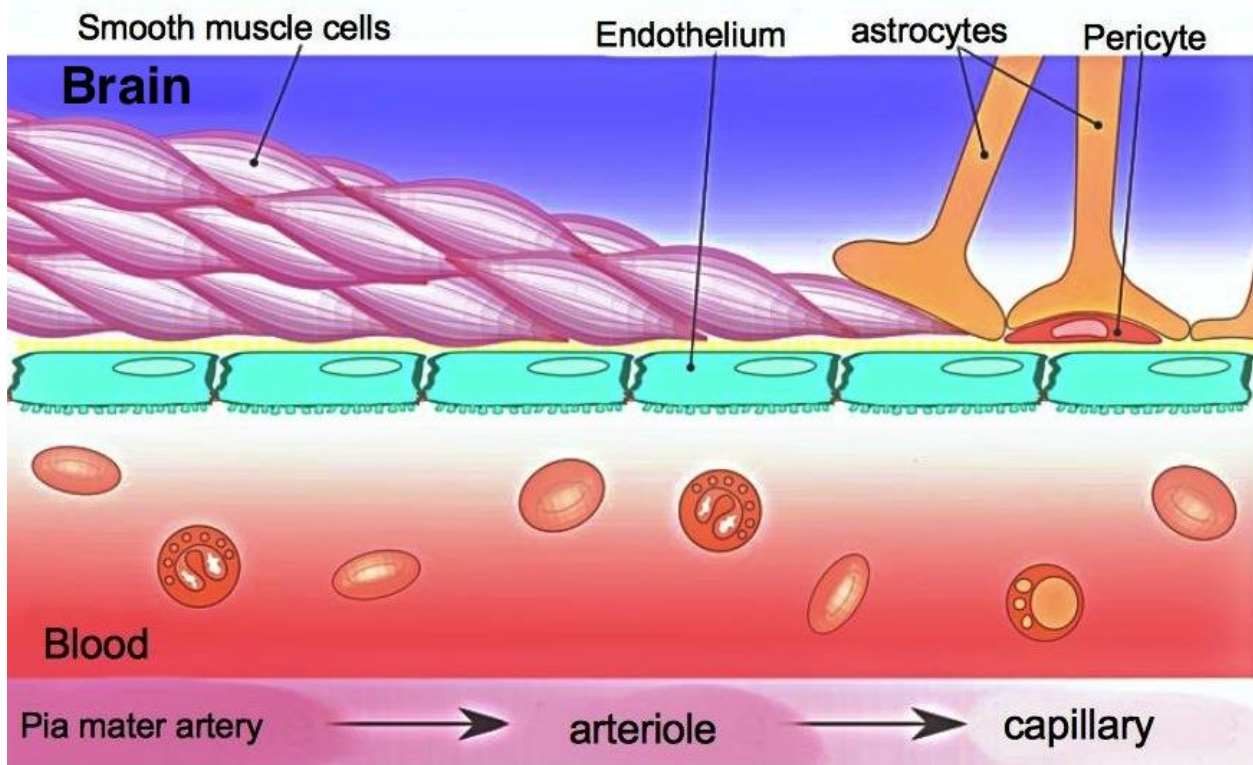


Figure 3.1. Constitution of blood vessels inside the brain [7]

The permeability is also affected by the shear stress that is imposed on the vessel wall from blood flow. Tight junctions are not formed unless the endothelial cells are under 0.3–2 Pa of shear stress, the standard level in brain capillaries [6,8]. Blood flows at approximately 6-12 nL/min through capillaries with diameters of 5-10 μm [6]. 3D printers do not have the capability to fabricate channels this small, so dimensions of the channel and properties of the fluid flow must be scaled up. It is important that the scaling must still provide the same shear stress as the *in vivo* environment.

3.2 Current Research

Because the environment surrounding the BBB is so complex, there are very few successful models. A study in 2016 showed only 10 reputable BBB-on-a-chip publications [8]. This number has increased but without consistent success for a standardized model [2]. Generally, drugs are tested with animals, which is considered the “gold standard” [8]. Testing with animals is an *in vivo* technique and is the most effective way of studying the complexity of the different environments. The movement and effect of drugs can be monitored as well as the animal’s reaction, instead of only the delivery success. *In vivo* animal studies tend to be expensive, difficult to perform, and have a high likelihood of displaying false results when transferring the drug to humans. *In vitro* models can include cells in a controlled environment but are often too simple to accurately re-create the environment being tested [8]. They have been found to be successful in determining single characteristics of drugs, like cytotoxicity, but not to test an entire system’s response to a drug [8].

BBB-on-a-chip devices could combine techniques from each previous method but there is not a standard method of doing so yet. Cells and tissue can be cultured in the device while also creating a similar environment using fluid flow. The models presented in the 2016 study all display similar difficulties and problems with standardization. The study states that the permeability of

the membrane model must be quantified in a way that all models, *in vivo* and *in vitro*, can be compared. Modes of transport other than diffusion can be present, so each model must account for this possibility when measuring permeability [8]. A better way to assess the permeability is the transendothelial electrical resistance (TEER), but not all models perform this test. The TEER is the “electrical resistance against paracellular transport,” which changes as the cell layer becomes tighter [8,9]. Incorporating electrodes into the device can make measuring the TEER an easy method of estimating the permeability of the membrane. A method of permeability assessment should be incorporated into the device design to provide the possibility of comparing to other models.

Cultured cells have presented many issues in the current BBB devices. As previously stated, all 3 types of cells (endothelial, astrocytes, and pericytes) should be included for a more accurate permeability. When all cells are included, the membrane has been found to be tighter in these devices. However, this membrane still causes unrealistic separation between the cells, which reduces the interactions between them [8]. Another difficulty is availability, as many models currently use animal cells. One study has successfully used neonatal rat cells in their device to create a permeability that is very similar to the *in vivo* environment, but the transferability to human testing is yet to be seen [10]. Human cells can be difficult to acquire and lose many crucial characteristics in the culture process [8]. Because of this difficulty, research is being performed to create better sources of these cells.

The final challenge in these models is exposing the cells and membrane to a standard shear stress. In normal *in vitro* models, tissue or cells are typically cultured in a petri dish or similar environment, without fluid flow around the cells. In comparison, many BBB models incorporate fluid flow so shear stress is inflicted on the membrane and cells. It is found that the shear stress is

beneficial to the membrane tightness since blood flow causes a similar shear stress *in vivo*. As devices become more standardized, the channels should be designed to apply a uniform shear stress across the membrane and cells at the same intensity as the *in vivo* environment [8].

3.3 Prior Work

The use of 3D printing was previously applied in Carlton McMullen's thesis, "Design, Fabrication, and Testing of a 3D Printer Based Microfluidic System." In his thesis, he developed microfluidic systems using 3D printing and conventional lithography techniques for molds with PDMS [11]. Both devices include micropumps and micromixers. He created a control system to test the effectiveness of each component and compared the two methods of fabrication [11]. McMullen also tested the surface of each material used, finding that Ninjaflex (used as structure material in 3D printing) is hydrophilic [11]. Because the material is hydrophilic, fluid is attracted to the surface and is less likely to form air bubbles in the microchannels, making it a suitable material for a microfluidic device.

The work presented in this thesis was developed using McMullen's findings on a 3D printed micropump using Ninjaflex. The micropump is operated by two chambers with a thin diaphragm separating them from the microchannel. Once filled with air, they deflect into the channel, pushing the fluid through the channel [11]. This interaction is shown in Figure 2. This micropump was tested at various frequencies of pneumatic actuation and air pressure to the diaphragms. McMullen determined a maximum fluid flow rate of 1120 $\mu\text{L}/\text{min}$ at a frequency of 10 Hz and pressure of 40 psi [11].

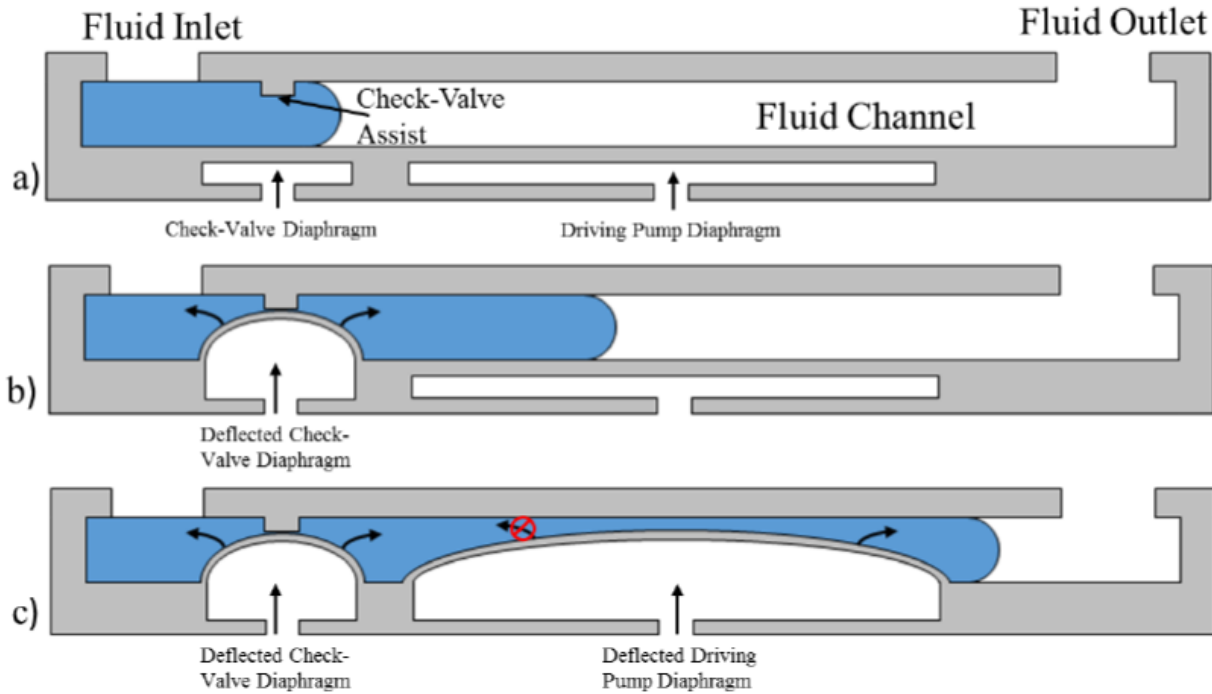


Figure 3.2. Pneumatical actuated diaphragm for micropump with flow indicated by arrows. (a) Diaphragms in initial position. (b) Small diaphragm deflected causing bi-directional flow. (c) Both diaphragms deflected with backflow prevented by check valve diaphragm. [11]

4 DESIGN, SIMULATION, AND FABRICATION

As stated in Section 3.2, many problems with current BBB-on-a-chip devices involve recreating the *in vivo* BBB environment in an *in vitro* device. One of the hardest parameters to recreate and measure is the shear stress imposed on the walls of the channel and the membrane. When increasing the size of the channel from the actual size of the brain capillary to the fabricated channel, the flow rate must also be changed to match the *in vivo* shear stress. This research first focused on determining the correct channel dimensions and flow rate to achieve a consistent wall shear stress of 0.3-2 Pa. The computational fluid dynamics module of COMSOL was used to test various dimensions and flow rates until this shear stress was achieved using water as the fluid. Prior to COMSOL simulations, theoretical calculations were performed to provide a basic insight to the type of flow and a theoretical flow rate required for different dimensions. Based on the

resolution of the 3D printer being used for fabrication, a minimum size for any feature of the device was established and considered for the simulations.

4.1 COMSOL Scaling Tests

To begin the experiment, COMSOL was used to accurately simulate fluid flow through channels of different sizes and shapes. There was a learning curve involved in the use of COMSOL, so to effectively use the program as a resource for designing the microchannels and operation parameters for the device, my own skill with the program was enhanced by verifying calculations corresponding to scaling the dimensions up from the brain capillary to the device's microchannel. Based on theoretical calculations, the COMSOL simulations were used to verify the flow rates for each channel. The theoretical calculations were completed using the equations below to determine flow characteristics of blood in the brain capillaries and match these in scaled up channels.

The two parameters that must equal when scaling up are the Reynolds number and shear stress. Because blood is typically identified as a non-Newtonian fluid [15], it cannot be represented using the COMSOL standard fluids. When scaling up to the device dimensions, water properties were used, instead, so that the flow could be simulated in COMSOL and evaluated more effectively in testing.

Initially, the values of density and dynamic viscosity of the blood and water is to be found. Then the kinematic viscosity and area is to be calculated. For the rectangular (scaled-up model) channel, the hydraulic diameter is to be found for Reynolds number calculations.

$$v = \frac{\mu}{\rho} \quad (1)$$

$$A_{BBB} = \frac{\pi D^2}{4} \quad (2)$$

$$D_H = \frac{2wh}{w + h} \quad (3)$$

$$A_{rectangle} = wh \quad (4)$$

Consequently, the volumetric flow rate (ft³/s) is to be calculated by multiplying the cross-sectional area and the flow velocity.

$$Q = V * A \quad (5)$$

The Reynolds number is the ratio of the inertial forces to the viscous forces. Subsequently, this formula is used to calculate the Reynolds number for both the BBB and the scaled-up model to check the status of the flow, which is either laminar or turbulent.

$$Re = \frac{u * L}{\nu} \quad (6)$$

Where L is the characteristic linear dimension (m) and u is the characteristic velocity of the fluid with respect to the object (m/s). This equation is simplified to the following equation, which can be used for pipe flow or a wide rectangular channel. For pipe flow like a brain capillary, the hydraulic diameter is just the diameter of the pipe and the area is the cross-sectional area. For a wide channel, the characteristic dimension, D_H, becomes the distance between the two wide plates, disregarding the width of the channel.

$$Re = \frac{Q D_H}{\mu A} \quad (7)$$

Finally, shear stress (Pa) for the BBB and the scaled-up model is to be calculated with the known values of volumetric flow rate, dynamic viscosity, and channel dimensions [8].

$$\tau_{BBB} = \frac{4 * \mu * Q}{\pi r^3} \quad (8)$$

$$\tau_{rectangle} = \frac{6 * \mu * Q}{w * h^2} \left(1 + \frac{h}{w}\right) * f * \left(\frac{h}{w}\right) \quad (9)$$

Equation 9 can be simplified based on the assumption that channel's width is much greater than the height. Equation 10 shows this simplification.

$$\tau_{rectangle} = \frac{6 * \mu * Q}{w * h^2} \quad (10)$$

First, a simulation was conducted using the dimensions of a brain capillary as a reference point. The simulation displayed a maximum velocity of $6.61 * 10^{-5}$ m/s, while calculations provided an average velocity of $4.77 * 10^{-5}$ m/s which is very close to the median velocity found in COMSOL. The Reynolds number for the flow through the brain capillary was calculated to be approximately 0.0025 using Equation 7. This is also used to match flow properties as the channel is scaled up. The actual size simulation results are shown below.

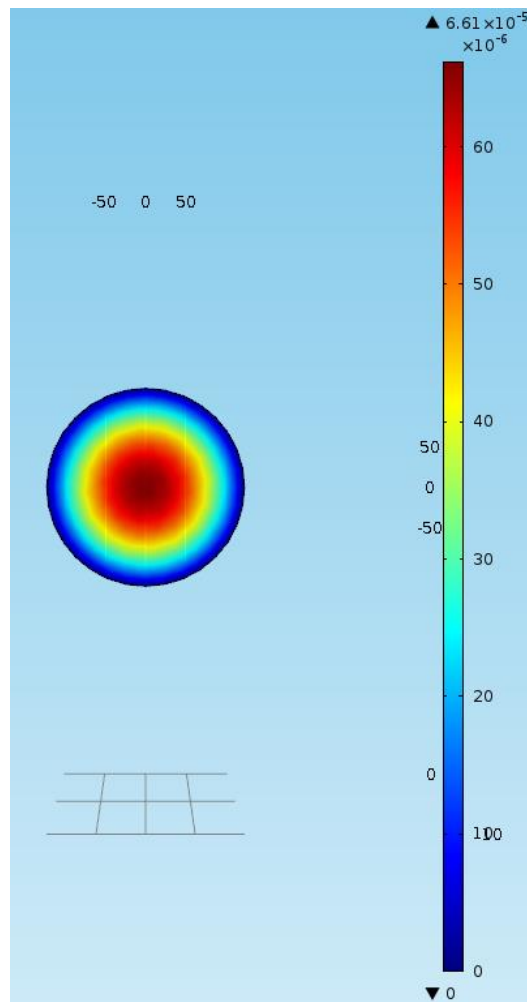


Figure 4.1. BBB velocity simulation results

The model was scaled up and simulated with different shapes of channels to determine the accuracy of theoretical calculations. A square and circular cross section channel was simulated with similar results to the actual size BBB cylinder. The table below provides velocity values for both methods for these test simulations.

Velocity Results	Excel (cm/s)	COMSOL (cm/s)
BBB dimensions	0.0477	0.047
Scaled up pipe flow BBB	15.45	15.43
Scaled up rectangular BBB	10.71	10.4

Table 4.1. Velocity measurements with theoretical calculations and COMSOL

4.2 COMSOL Shear Stress

Once the simulations were providing sufficient results based on the velocity calculations, flow was simulated through multiple channel options for the microfluidic device. The options had 2 constraints that had to be met: the shear stress must be uniform across the final location of the membrane and it must be within 0.3-2 Pa. The uniformity was achieved by designing the channels with rectangular cross-sections, where the membrane would be included on the larger face. To meet the range of shear stress values, the flow was analyzed. In the brain capillary, the Reynolds number was calculated to be 0.0025 using average size and flow values [14], meaning it qualifies as Stokes flow ($Re \ll 1$), which means the viscous forces become larger in comparison to the inertial forces [12]. In typical laminar and turbulent flow, the condition is the opposite. The flow through the device was, then, desired to be as close to Stokes flow as possible.

Using Excel Solver, theoretical calculations were quickly performed to find ideal height and width dimensions for the channel, while attempting to match the *in vivo* shear stress and Reynolds number. By setting the width to equal 1.6 mm, the height to equal 0.2 mm, and the flow

rate to equal 700 $\mu\text{L}/\text{min}$, the theoretical shear stress was approximately 0.76 Pa, which would satisfy the desired range. These dimensions were tested and found to have similar results from COMSOL. The shear rate across the channel is shown in the figures below. Shear stress is not shown as a result in COMSOL simulations, so Equation 11 is used to calculate the wall shear stress.

$$\tau = \dot{\gamma} * \mu \tag{11}$$

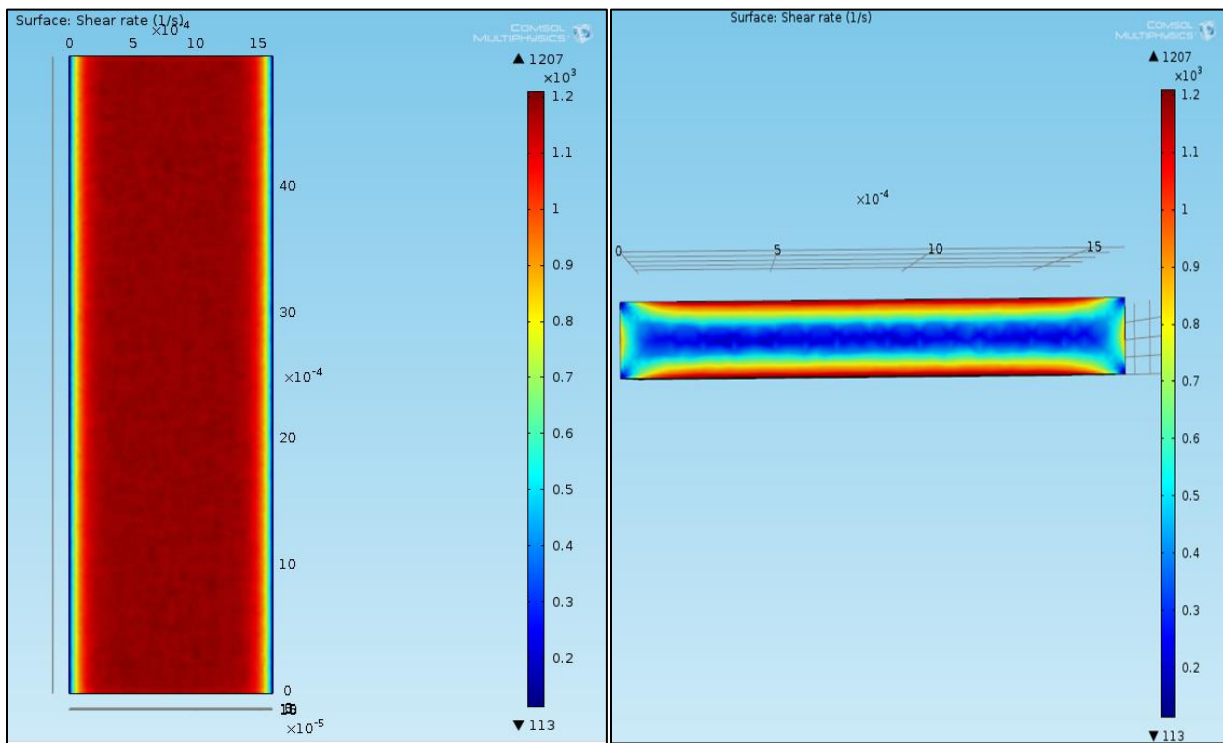


Figure 4.2. (Left) Shear rate across top face of channel; (Right) Shear rate at inlet of channel

This shear rate corresponded to a shear stress of 0.84 Pa, satisfying the range of values. Unfortunately, the 3D printer was unable to print features at 0.2 mm, so the dimensions had to be increased. This successful simulation, though, proved that the required shear stress could be met in the device with more testing.

To accommodate the 3D printer’s resolution, the smallest dimension of the channel could not be lower than 0.5 mm. So, the simulation was run again using a channel with a height of 2 mm and a width of 0.5 mm. Beginning with 2502 $\mu\text{L}/\text{min}$ for the flow rate, COMSOL displayed a shear stress of 0.43 Pa. This was within the range of shear stress values, but the flow rate was well above the maximum flow rate determined by McMullen using the 3D printed micropump, which was 1120 $\mu\text{L}/\text{min}$. Two more simulations were performed to find the range of flow rates to meet the shear stress range. The following graph displays these results. The shear stress remained uniform across each wall with the increase in size.

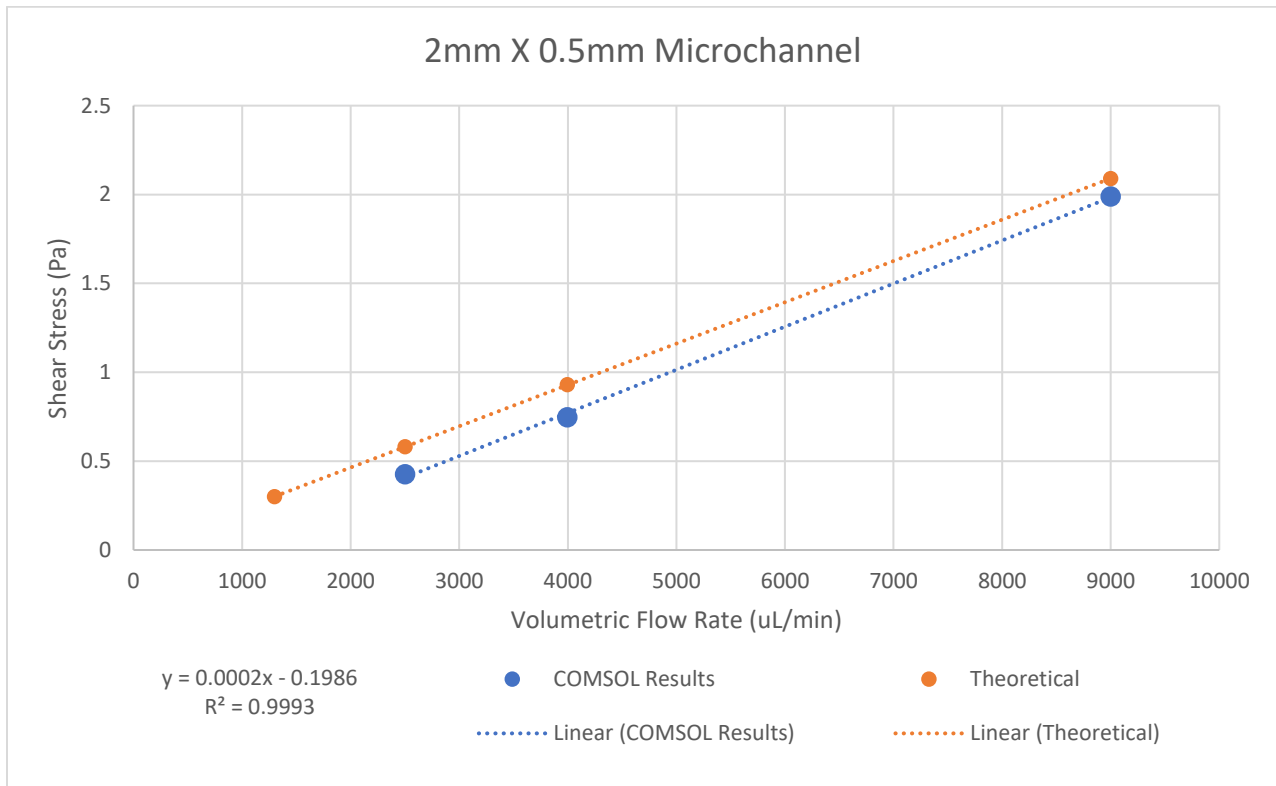


Figure 4.3. Wall shear stress at each simulated flow rate

To perform the COMSOL simulations, each model was created as a 3D component. A stationary study was used with Laminar Flow added as physics. The density and viscosity of water were used for all models because water will be used through the BBB-on-a-chip device. The flow was defined by the volumetric flow rate found in the theoretical calculations. A simulation was

performed at approximately 2502 $\mu\text{L}/\text{min}$, 4000 $\mu\text{L}/\text{min}$, and 9000 $\mu\text{L}/\text{min}$ to observe the range of shear stress values, as stated previously. Based on the data presented in Figure 4.3, the trendline in the lower right corner can be used to determine the minimum flow rate required for the minimum shear stress allowed, since this simulation was not completed. It is found to be very close to the first simulation, as 2493 $\mu\text{L}/\text{min}$ equates to 0.3 Pa of shear stress on the channel walls. The parameters of each COMSOL simulation and results are available in the table in Appendix A.

Figure 4.3 also includes theoretical shear stress calculations that were compared to the COMSOL results, which can be seen in orange. The theoretical results found that the shear stress could be higher than the COMSOL results which would improve the effectiveness of this device. The hydraulic diameter was used for the rectangular channel with Equation 8 to determine these results for water flow through the microchannel. The largest difference is shown as the minimum required flow rate is only 1300 $\mu\text{L}/\text{min}$ to reach the required shear stress value of 0.3 Pa. However, the COMSOL results are utilized for design purposes for the rest of this research.

The following image was the first successful COMSOL simulation in terms of the correct shear stress. The volumetric flow rate was 2502 $\mu\text{L}/\text{min}$, resulting in the shear stress found in Figure 5, 0.43 Pa. The simulation indicated the wall shear stress on the wide face on the channel will still be uniform even though the size of the channel was increased to accommodate the 3D printing resolution.

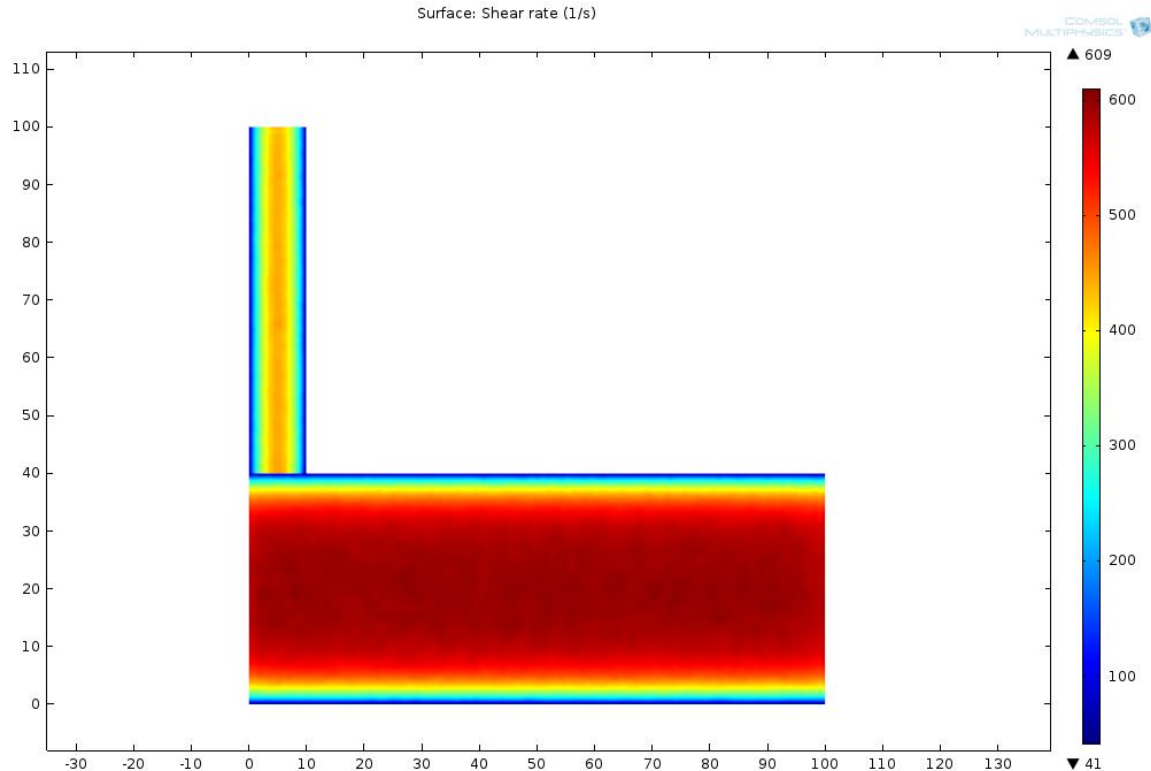


Figure 4.4. Shear rate of 2 mm by 0.5 mm channel at 2502 $\mu\text{L}/\text{min}$

4.3 3D Prints

A MakerBot Replicator 2 printer with NinjaFlex as material was used for all prints. All designs were modeled in Solidworks and saved as .STL files. The .STL files were opened in Replicator G and converted to a G code for the printer to read. All prints were set to 100% infill, 220°C print temperature, and feed rate and travel feed rate both set to 20 mm/s. The layer height was originally set to 0.15 mm but changed to 0.08 mm to improve the print quality. These parameters were specified when creating the G code. Multiple prints were completed for the testing process of this research. McMullen’s original micropump design is displayed below in Figure 6. This figure highlights the use of the diaphragms for pumps with compressed gas. It also displays the basic channel configuration used in each device fabricated and tested for this research. Each 3D design and completed print are discussed in further detail in sections 5.2.1 – 5.2.4 of the Results section.

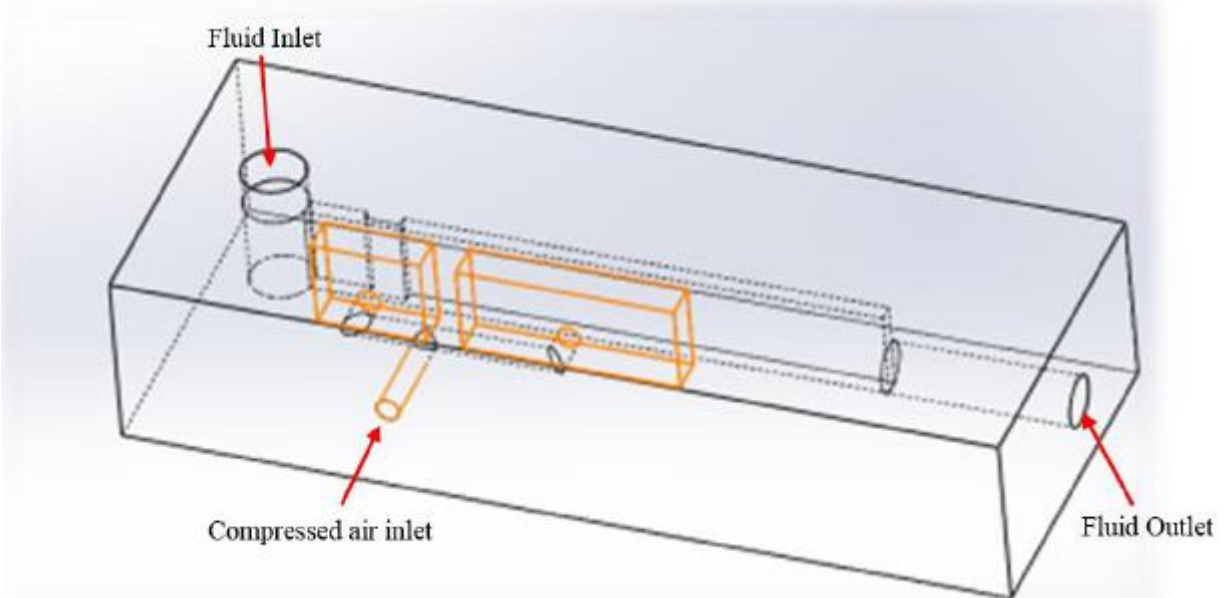


Figure 4.5. “3D model of 3D printed micro-pump. The orange lines indicate the location of the air inlet, and air-chamber aligned to the diaphragms” [11]

5 RESULTS/DISCUSSION

5.1 Micropump Test Setup

Prior to printing the entire device, the micropump and microchannel were printed to further test the capabilities of the micropump. In McMullen’s work, he found the maximum flow rate of $1120 \mu\text{L}/\text{min}$ at 40 psi and 10 Hz. Because the COMSOL simulations suggest a much higher flow rate is required to match the shear stress, alterations were made to the pump parameters and tested. McMullen’s method of measuring flow rate was utilized in this research. For all devices, the flow rate was determined by measuring the distance the fluid had traveled through Tygonthane tubing from the outlet of the device. A pipette tip was inserted to the inlet of the device, where water was dropped in to prime the device. The outlet tubing was raised to the water level in the pipette tip to remove gravitational forces acting on the water so the pump would be the only source for flow. A ruler was used to measure the distance the water travels through the outlet tube. The lab setup is shown in the picture below.

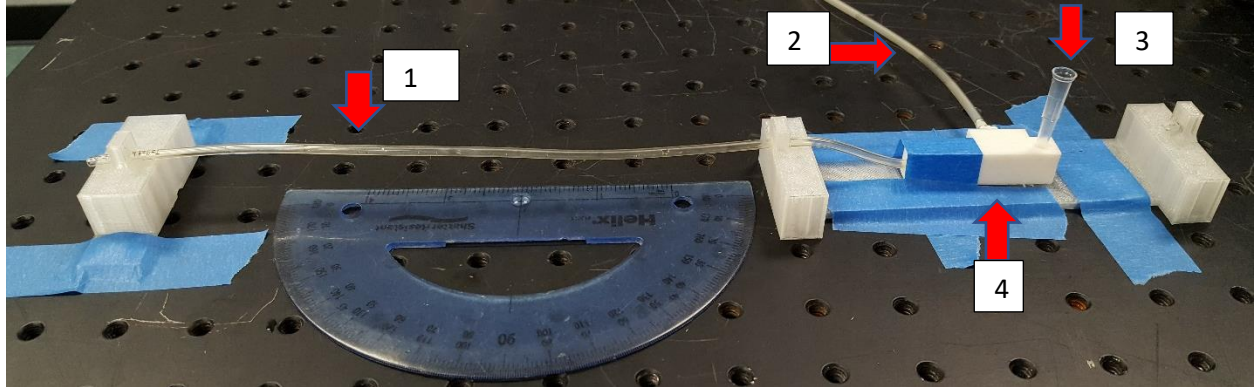


Figure 5.1. (1) Section of tubing used to measure flow rate with ruler; (2) Inlet tubing for compressed gas; (3) Pipette tip for fluid inlet; (4) Taped and secured micropump device – in white.

To measure the flow rate, the displacement of the water was measured using the ruler and the time was defined in the control system. Using the following equation, this information was translated to the velocity of the fluid.

$$V = \frac{\Delta x}{\Delta t} \quad (12)$$

Using the velocity of the fluid and the cross-sectional area of the tubing, the volumetric flow rate was determined and used to compare to McMullen's findings.

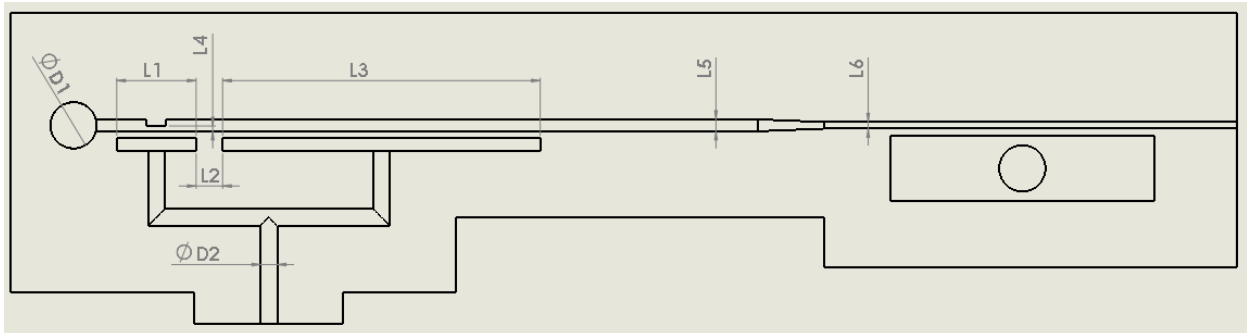
$$Q = V * A \quad (13)$$

Each pump that was tested utilized this testing procedure. However, many improvements were made throughout the research. After each trial, which consisted of priming the system and allowing the pump to run for one 5 second interval, completely cleaning out the entire system was attempted. This was not always possible, but after several unsuccessful trials, it was found that with less air pockets throughout the system, the water flowed with less resistance. The outlet tubing was also cut at the minimum possible length to still measure velocity because excess tubing caused more backpressure on the pump, creating more resistance to the flow. The pump also caused a large amount of initial back flow but this is believed to be due to the first stroke of the pump diaphragm not preventing backflow.

5.2 Micropump Results

Throughout this research, several micropump designs were printed and tested. Based on the COMSOL simulation results, the required volumetric flow rate would need to be much larger than that achieved in McMullen's research. Because of this, the first pump (Test Pump 1) that was printed included diaphragms twice the size of those designed by McMullen. The second pump (Test Pump 2) that was tested was McMullen's design. The third pump (Test Pump 3) only made slight changes to the second, including filleting edges inside the microchannels and reducing the layer height of the 3D printer to improve the print quality. The third pump was very successful, so the fourth test pump (Test Pump 4) was modified to a horizontal inlet and included a section of the microchannel at the dimensions determined from the COMSOL simulation, 2 mm by 0.5 mm. Until this point, all microchannels were 5 mm by 0.9 mm because that was the height of the pump diaphragms and to cause less resistance to the flow. This pump was unsuccessful so the length of the entire device and, more importantly, the smaller channel section was reduced to reduce the backpressure. After these modifications, Test Pump 5 was fabricated and printed, but did not have success.

5.2.1 Test Pump 1



Label	Dimension (mm)
L1	6.0
L2	2.0
L3	24.0
L4	0.50
L5	0.90
L6	0.50
D1	3.50
D2	1.25

Figure 5.2. Test Pump 1 top view of cross section, with dimensions

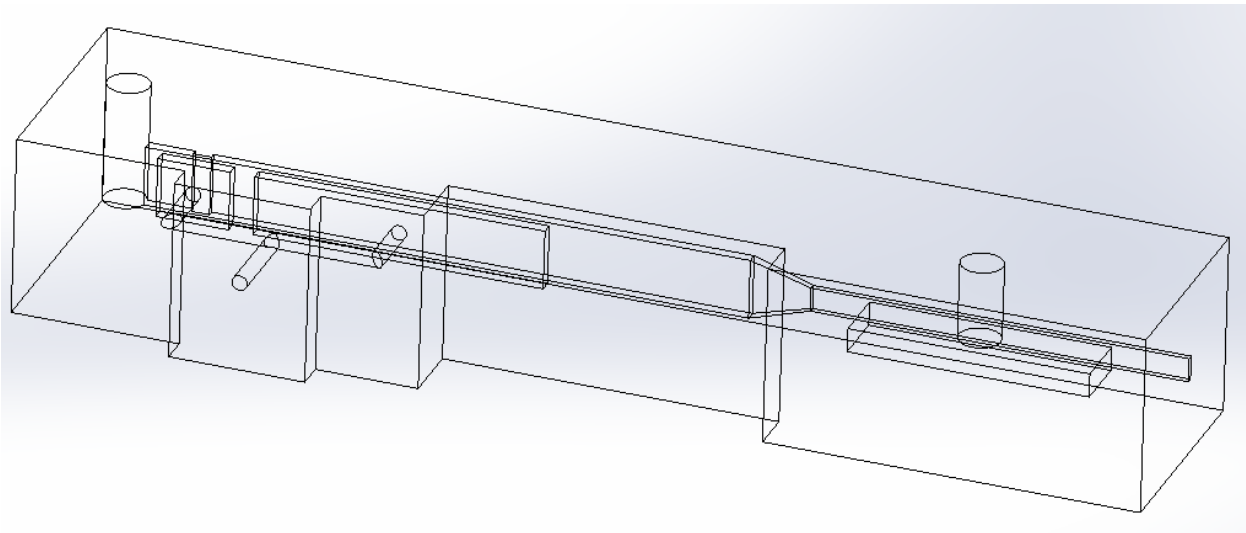
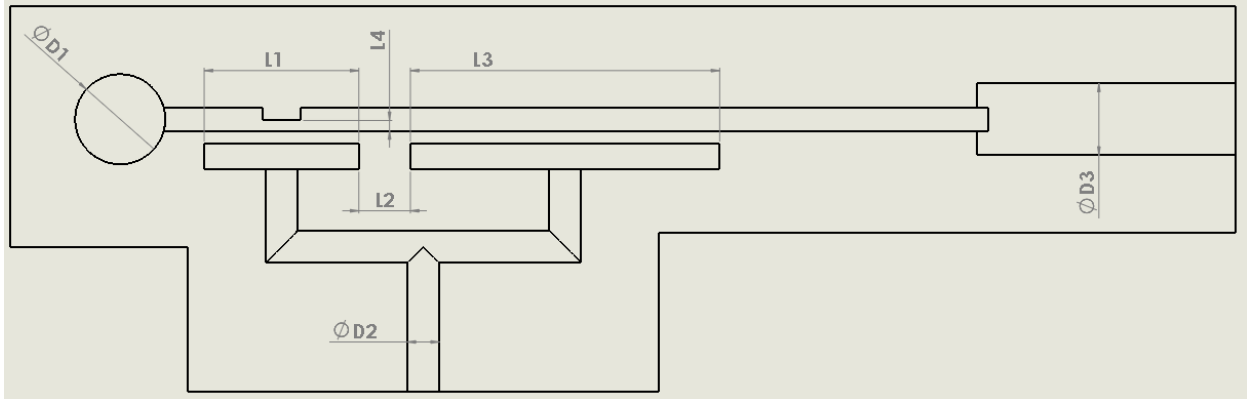


Figure 5.3. Isometric view of Test Pump 1

Test Pump 1 began as an optimistic prototype for the entire BBB-on-a-chip device. The outlet channel was designed with the dimensions found through the COMSOL simulations that were required for the membrane (to be added at a later date) to be under the correct shear stress. A separate reservoir was fabricated next to this channel to symbolize the accessibility to the membrane and the location for cell culturing and BBB-characteristic testing. The size of the second diaphragm in the pumping mechanism was doubled to accommodate the larger required flow rate. Since the necessary flow rate calculated from COMSOL was larger than McMullen's results, this device was meant to test the possibility of increasing the flow rate by enlarging the pump diaphragm.

This device proved to be unsuccessful. Flow was not produced through the device, which could be due to two different issues. The length of the smaller section of the main channel was unnecessarily long and caused a large amount of backpressure to the pump. The enlargement of the pump diaphragm did not help in increasing the flow rate since it was unable to produce any flow.

5.2.2 Test Pump 2



Label	Dimension (mm)
L1	6.0
L2	2.0
L3	12.0
L4	0.50
D1	3.5
D2	1.25
D3	2.8

Figure 5.4. Test Pump 2 top view of cross section, with dimensions

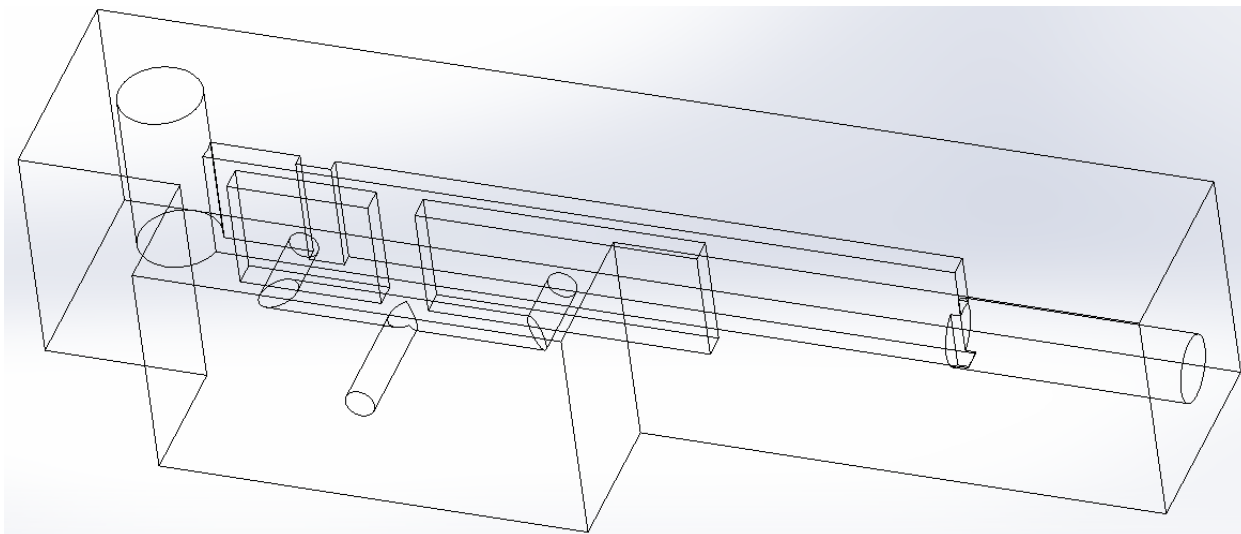


Figure 5.5. Isometric view of Test Pump 2

Test Pump 2 had the exact dimensions defined by McMullen in his final micropump. The purpose of printing this pump was to gain more data to support McMullen's results. By ensuring that flow could be consistently produced with this pump, components of Test Pump 1 could be incorporated one at a time, instead of starting with a completely new device and being unsure of the root cause of no flow. Unfortunately, this pump only worked for 5-10 trials before it began to leak through the diaphragms and bottom of the device. This leaking suggested the quality of print was not sufficient. This issue was fixed with the fabrication of Test Pump 3. The cleaning system was implemented while testing this pump, because after several trials, the air pockets in the outlet tubing seemed to slow the flow. The graph below includes volumetric flow rate results from the first 5 trials with Test Pump 2. After these trials, the pump began to leak substantially, causing the switch to Test Pump 3.

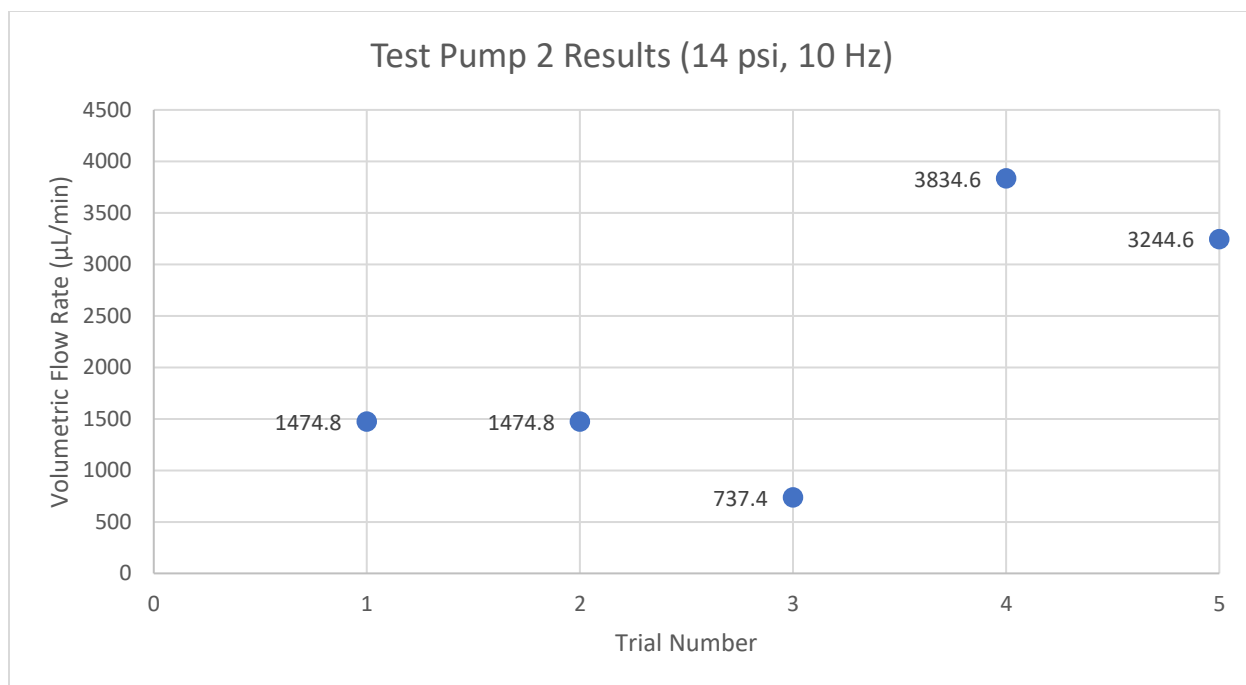


Figure 5.6. Test Pump 2 flow rate results

The results were very inconsistent, but this was a small number of trials. After the third trial, the cleaning and priming process was improved, as discussed in section 5.1. This caused an increase in flow rate. Because these flow rates were within the range of flow rates discovered in section 4.2, the current micropump design was determined a sufficient component for the full BBB-on-a-chip model. However, sufficient data to fully support this conclusion was not taken with this pump due to leakage, so Test Pump 3 was produced.

The flow rate results found using Test Pump 2 were measured using the methods described in section 5.1. All trials were set to a pressure of 14 psi and a frequency of 10 Hz for the pump activation.

5.2.3 Test Pump 3

Test Pump 3 uses the same design as Test Pump 2, but the 3D printing parameters were altered to improve the quality of print and prevent leaking. The layer height for each print had been originally set to 0.15 mm but was reduced to 0.08 mm. By reducing the layer height, the

print features can be more precise, improving the quality of the pump diaphragms and microchannels. Once the leaking was fixed by reducing the layer height, Test Pump 3 was successful in gathering flow rate data at various pressure settings for the pump operation. Trials were completed at a frequency of 10 Hz and pressures of 20 psi, 30 psi, and 40 psi, with flow rate results consistently above those discovered by McMullen. Less operational settings were tested than McMullen's research, simply because the ability to produce a higher flow rate was more important than being able to predict the exact flow rate (for the time-being). Ideally, once the entire BBB-on-a-chip device is fabricated and successful, this portion of the experiment would be completed again to define operational parameters required for different flow rates.

The results of each pressure setting are displayed in the following graphs. As previously stated, the main objective was to prove that 2500 $\mu\text{L}/\text{min}$ was consistently possible, which was achieved. All settings produced an average flow rate above this mark, further validating this pump's capability of operating the BBB-on-a-chip device.

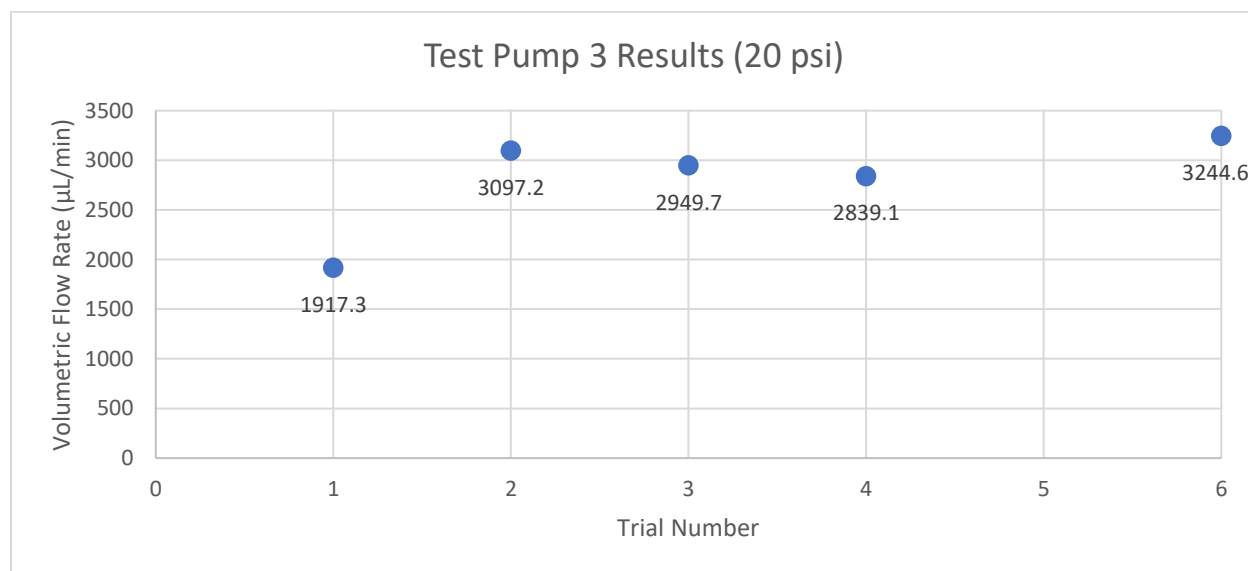


Figure 5.6. Test Pump 3 results at 20 psi

The first set of trials were completed at a pressure of 20 psi, and resulted in an average flow rate of 2810 $\mu\text{L}/\text{min}$. The first trial was slightly low but the most likely cause is ineffective priming. This trial was one of the first test runs and, as stated, the priming and cleaning required a learning curve to work effectively. Trial 5 also had issues with cleaning and priming, causing no flow through the device.

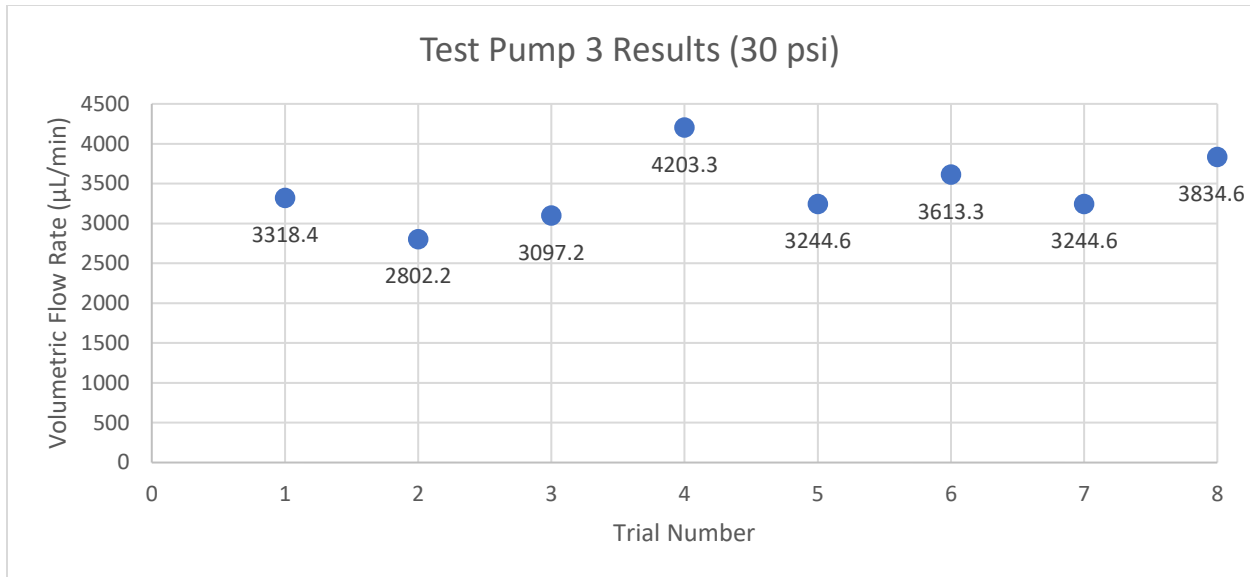


Figure 5.7. Test Pump 3 results at 30 psi

Trial runs with the pressure set to 30 psi displayed similar results to those at 20 psi, but with an average flow rate of 3420 $\mu\text{L}/\text{min}$. At this setting, most trials showed the flow beginning to slow before the 5 seconds had expired, likely due to the inlet reservoir running out of water. This was more prevalent during the trials with 40 psi of pressure. To improve this problem, the trial time is reduced to 3 seconds, which showed more accurate results. Because the inlet was depleted of water after a shorter period of time, the same displacement of water was caused in less time. By reducing the trial time, the actual velocity could be determined since the water was moving for the entire test. Again, the testing procedure became more uniform as more were completed, and the flow rate began to converge to an average value of 5235 $\mu\text{L}/\text{min}$.

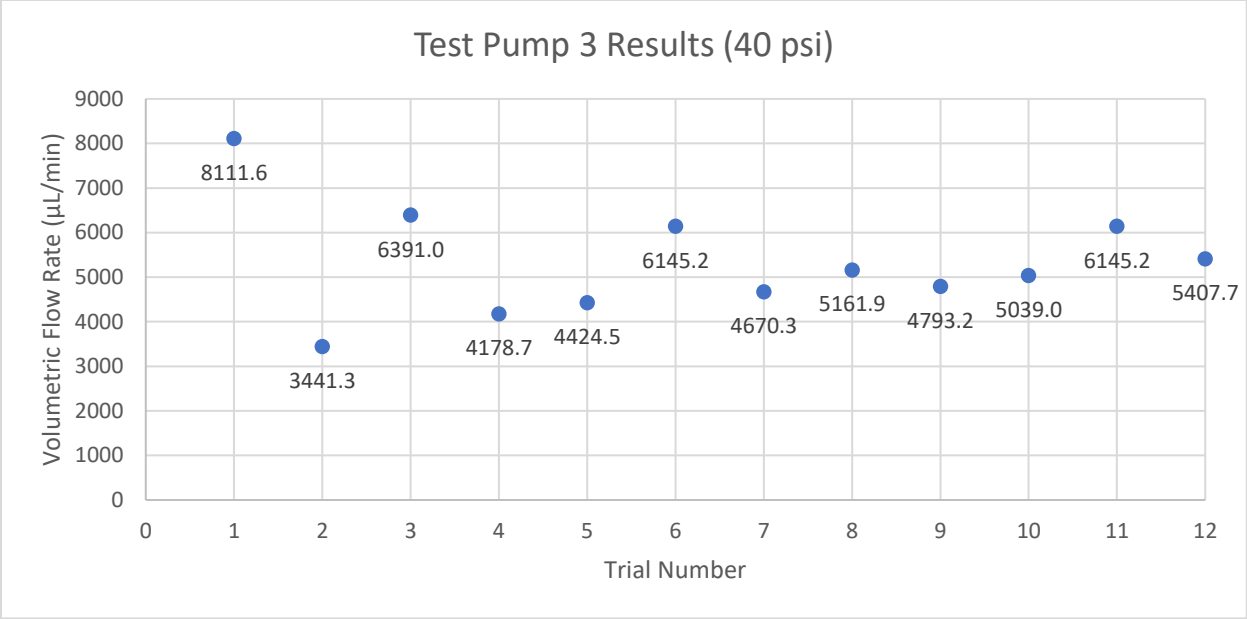


Figure 5.8. Test Pump 3 results at 40 psi

Based on these tests, a sample of the possible shear stress values can be calculated based on the average flow rate at each pump actuation pressure. The actuation frequency remained constant but could be tested for each pressure value in the future. The graph below shows the required pump actuation pressure for different shear stress values based on these average flow rates. However, the flow rates were not constant, so the flow rate should still be measured to get a more exact prediction of the shear stress inflicted on the channel walls.

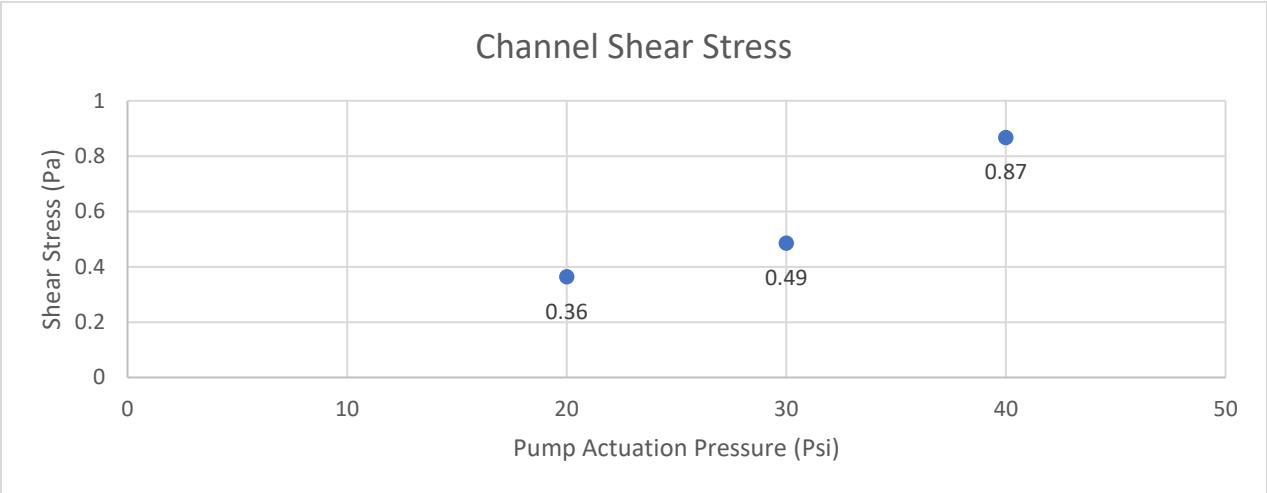


Figure 5.9. Applied shear stress on microchannel walls at each pump actuation pressure

5.2.4 Test Pumps 4 & 5

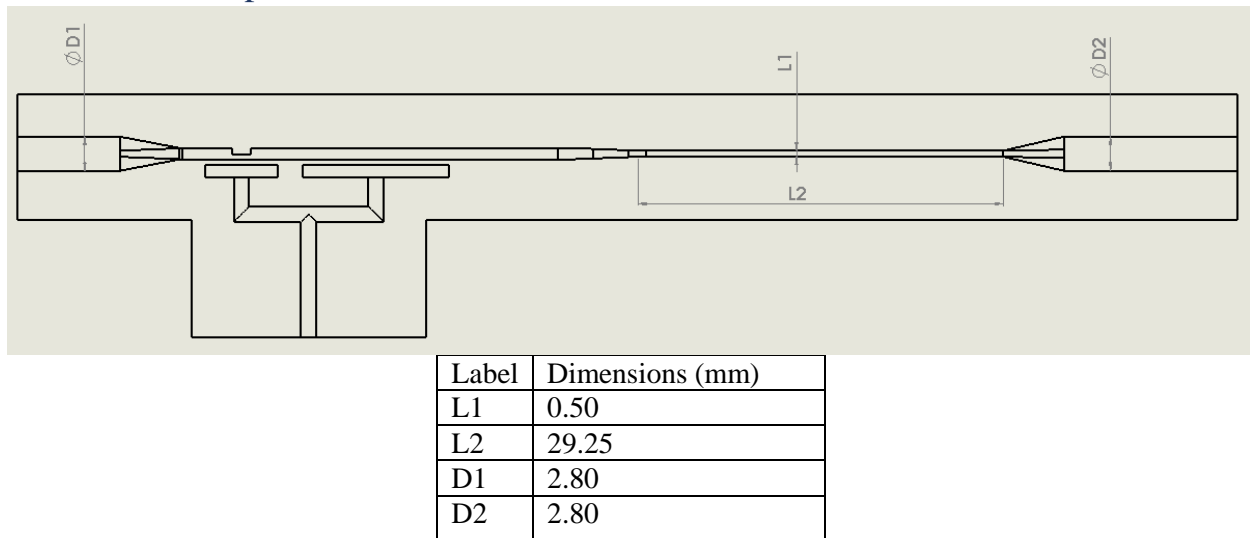


Figure 5.10. Test Pump 4 top view of cross section, with dimensions

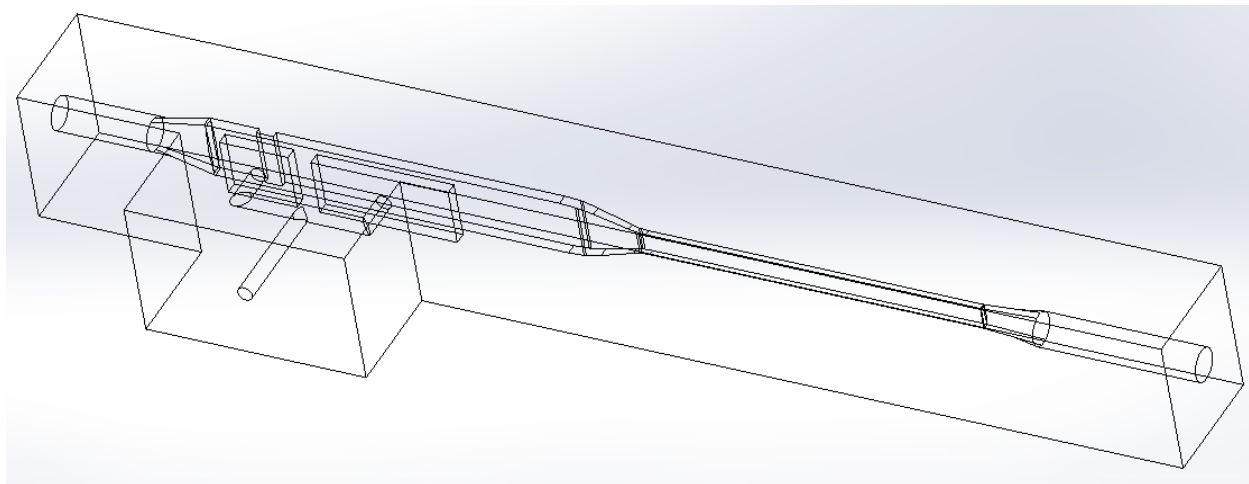


Figure 5.11. Isometric view of Test Pump 4

Test Pump 4 was designed to incorporate the dimensions of microchannel required for the shear stress range that were determined from COMSOL with the successful micropump from Test Pump 3. It also included a horizontal inlet instead of vertical, to test the possibility of a longer trial time. With a horizontal inlet, a reservoir system using petri dishes could be put in place to

pump water from one dish to another, instead of testing with a very small amount of water for only 5 seconds.

Fluid flow was not produced by Test Pump 4, as air was only pushed out the inlet and outlet. This was believed to be due to a large amount of backpressure caused by the long section of microchannel with smaller dimensions. This was one possible cause for lack of flow in Test Pump 1, as well. However, this was attempted to be resolved with Test Pump 5, by reducing the length, but Test Pump 5 was also unsuccessful at producing fluid flow. The dimensions and design of Test Pump 5 is shown below.

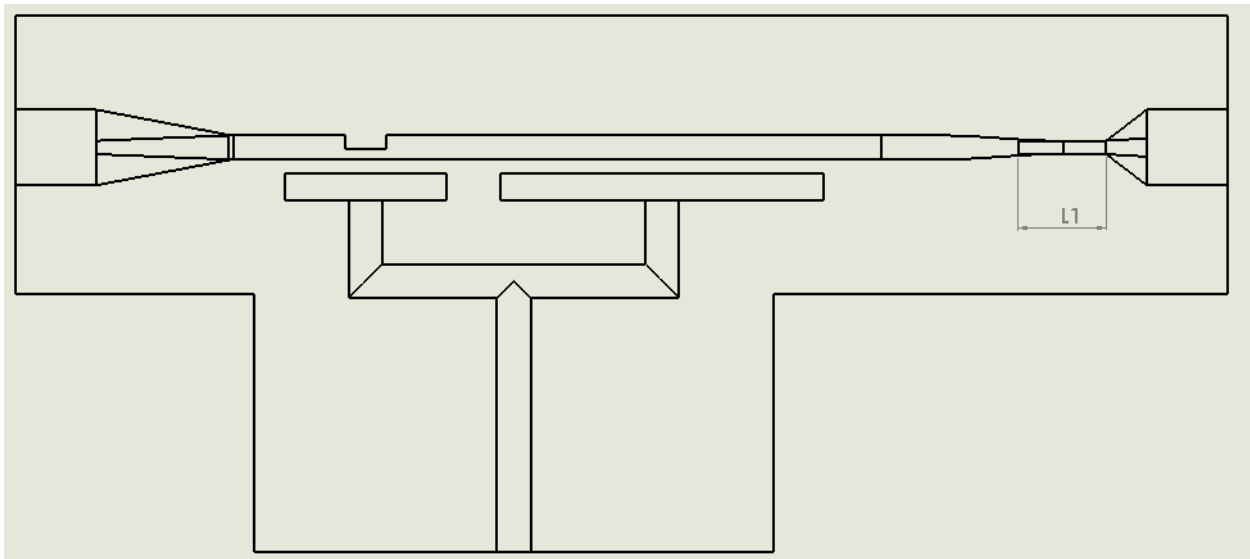


Figure 5.12. Test Pump 5 top view of cross section

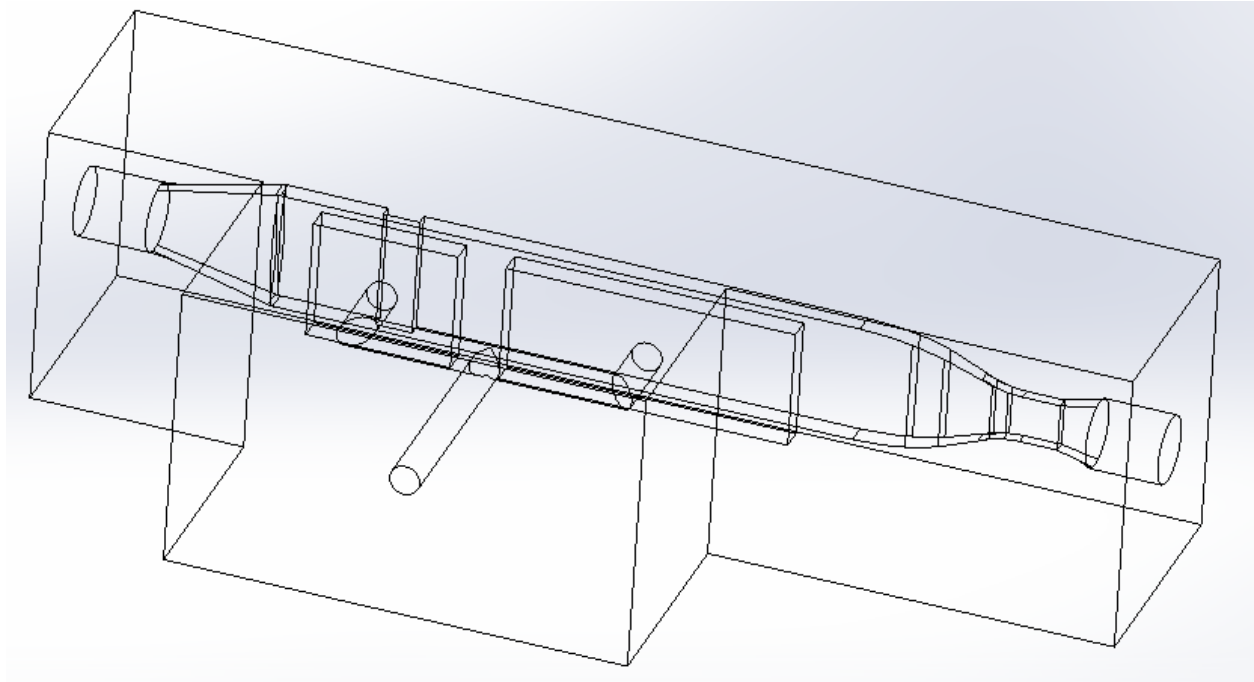


Figure 5.13. Isometric view of Test Pump 5

After unsuccessful attempts at producing flow with Test Pumps 4 and 5, it was found that reducing the length of the microchannel with smaller dimensions was not the main cause of no fluid movement. Both systems utilized the testing setup shown below in Figure 20. Based on these results, the horizontal inlet is the suspected problem. The inlet reservoir consists of a petri dish that the inlet tubing must travel over the wall and back down into the dish to the water level, so the pump must pull the fluid above the wall of the petri dish. In all previous tests, gravitational force serves to force water towards the pump diaphragms. More specifically, the gravitational force defines the direction of the small amount of flow during the pump's suction stroke, or when the diaphragms are returning to the original position. The displacement caused by the diaphragms must be replaced as they move back to the original position, and without gravitational force, the water is pulled back from the inlet and outlet, instead of supplying the pump with more water from the inlet. Because of this, the inlet must be vertical to continuously send fluid to the pump diaphragms.

6 CONCLUSIONS

This research successfully determined dimensions and actuation parameters for a 3D printed BBB-on-a-chip microfluidic device. COMSOL simulations were used to predict the incident shear stress on the walls of microchannels at different flow rates. The dimensions of the microchannel were modified to reach the bounds of the shear stress range of the *in vivo* BBB at achievable flow rates. This was based on Carlton McMullen's findings on a maximum flow rate produced by a 3D printed micropump. However, the simulated microchannel required flow rates much higher than the maximum McMullen defined.

The minimum shear stress was predicted to occur as a flow rate higher than McMullen's but it was believed to be attainable. After several failed micropump models, McMullen's design was used to find produce an average volumetric flow rate of 5235 $\mu\text{L}/\text{min}$, easily within the range of flow rates required for the range of shear stress values, which was found to be approximately 2500-9000 $\mu\text{L}/\text{min}$. The maximum flow rate was produced with an actuation pressure of 40 psi and actuation frequency of 10 Hz. This finding suggests this micropump is capable of operating a BBB-on-a-chip device.

Once the micropump was found to be successful, the smaller channel to test the BBB was added to the design, along with a horizontal inlet, which would be more realistic for a fully-functional device. The new design did not function properly, as the micropump was unable to produce a flow rate from the horizontal inlet. Based on these findings, a new design for an inlet reservoir must be produced if the horizontal inlet is to remain in the design.

7 FUTURE WORK

The primary goal of this research is to produce a microfluidic device that would produce conditions similar to those around the BBB using 3D printing and water as the fluid. The micropump has proven capable of the required flow rates and the dimensions of a microchannel

that can accurately replicate the *in vivo* shear stress imposed on the BBB. The inlet and outlet system for the device should be redesigned to produce continuous flow through the device while eliminating flow due to gravity. More specifically, a controlled method of continuously supplying fluid to the pump should be found.

The micropump's flow rate capabilities should also be investigated further. During this research, the actuation pressure was changed, but the actuation frequency was held constant because lower frequencies seemed to produce greater flow rates after initial investigation. Now that this micropump will be used for the BBB-on-a-chip device, the average flow rate at different frequencies should be measured at the previously defined actuation pressures.

Once the system is functional, alternate fluids should be introduced and tested to move closer to the fluid properties of blood. This will help to better simulate the environment with the physical characteristics that are created with this research. This will also be necessary for the introduction of cells so that the cell culturing process can begin. Also prior to cell culturing, methods for measuring permeability, such as TEER measurements, should be implemented. Components for these measurements should be included in the final design so that once cells are introduced, all aspects of the membrane can be investigated. The BBB membrane in the microchannel must be tested with cells and a more realistic fluid for permeability.

8 REFERENCES

- [1] A. Wolff, M. Antfolk, B. Brodin and M. Tenje. In Vitro Blood-Brain Models – An Overview of Established Models and New Microfluidic Approaches. *Journal of Pharmaceutical Sciences*. 104, pp. 2727-2746. 2015.
- [2] J. Madhusoodanan. Designing In Vitro Models of the Blood-Brain Barrier. *TheScientist*. Web. 2016.
- [3] Casquillas, G. V. and Houssin, T. Introduction to Lab-on-a-Chip 2015: Review, History and Future. *Elveflow*. Web. 2015. <http://www.elveflow.com/microfluidic-tutorials/microfluidic-reviews-and-tutorials/introduction-to-lab-on-a-chip-2015-review-history-and-future/>
- [4] Ho, C., Ng, S., Li, K., & Yoon, Y. (n.d.). 3D printed microfluidics for biological applications. *Lab Chip*, 3627-3637.
- [5] P. N. Nge, C. I. Rogers and A. T. Woolley, *Chem. Rev.*, 2013, 113, 2550–2583.
- [6] Wong, A. D., Ye, M., Levy, A. F., Rothstein, J. D., Bergles, D. E., & Searson, P. C. (2013). The blood-brain barrier: an engineering perspective. *Frontiers in Neuroengineering*, 6, 7. <http://doi.org/10.3389/fneng.2013.00007>
- [7] Schematic sketch showing constitution of blood vessels inside the brain. *Wikimedia Commons*. Armin Kübelbeck. March, 2009.
- [8] Helm, Marinke W Van Der, Andries D Van Der Meer, Jan C T Eijkel, Albert Van Den Berg, and Loes I. Segerink. *Microfluidic Organ-on-chip Technology for Blood-brain Barrier Research*. *Tissue Barriers*. Taylor & Francis, 2016. Web. 14 Dec. 2016.
- [9] Thuenauer R, Rodriguez-Boulan E, Romer W. Microfluidic approaches for epithelial cell layer culture and characterisation. *Analyst* 2014; 139:3206-18; PMID:24668405; <http://dx.doi.org/10.1039/C4AN00056K>
- [10] S. Deosarkar, B. Prabhakarandian, B. Wang, J.B. Sheffield, B. Krynska, M. Kiani. A Novel Dynamic Neonatal Blood-Brain Barrier on a Chip. *PLOS ONE*, 2015, DOI: 10.1371/journal.pone.0142725
- [11] McMullen, Carlton. Design, Fabrication, and Testing of a 3D Printer Based Microfluidic System. *MSME Thesis*. University of Arkansas. 2015.
- [12] Kirby, B.J. (2010). *Micro- and Nanoscale Fluid Mechanics: Transport in Microfluidic Devices*. Cambridge University Press. ISBN 978-0-521-11903-0.
- [13] Melinda Wenner Moyer. *Organs-on-a-Chip for Faster Drug Development*, *Scientific American*. 25 February 2011
- [14] Wong, A. D., Ye, M., Levy, A. F., Rothstein, J. D., Bergles, D. E., & Searson, P. C. (2013). The blood-brain barrier: an engineering perspective. *Frontiers in Neuroengineering*, 6, 7. <http://doi.org/10.3389/fneng.2013.00007>

9 APPENDICES

9.1 Appendix A – COMSOL Parameters and Results

Test	Channel Height (mm)	Channel Width (mm)	Channel Length (mm)	Inlet Flow Rate ($\mu\text{L}/\text{min}$)	Inlet Pressure (Pa)	Outlet Pressure (Pa)	Shear Stress (Pa)	Within Shear Stress Range (Y/N)
1	0.5	5	25	2500	n/a	1300	0.154	N
2	0.5	5	25	n/a	4000	1300	0.2359	N
3	0.5	8	25	n/a	4000	1300	0.2331	N
4	8	0.5	25	2500	n/a	1300	0.0938	N
5	10	0.5	50	2500	n/a	1000	0.0728	N
6	2	0.5	50	2500	n/a	1000	0.45	Y
7	2	0.5	50	4000	n/a	1000	0.75	Y
8	2	0.5	50	9000	n/a	1000	1.99	Y
9	2	0.5	5	2500	n/a	1000	0.43	Y

Table A.1. COMSOL Testing parameters and results (Inlet flow rate OR pressure was required for the simulation)

9.2 Appendix B – 3D printed models

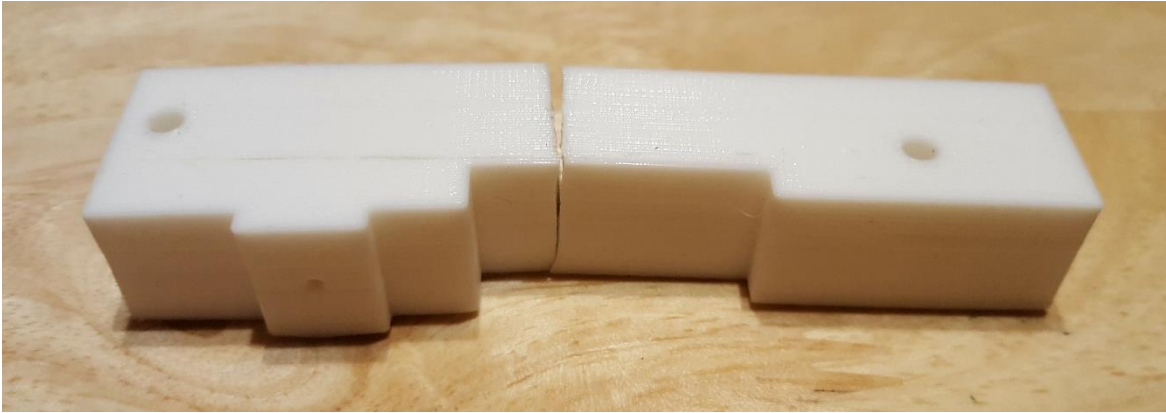


Figure A.2. Test Pump 1 (cut in half to investigate problems)

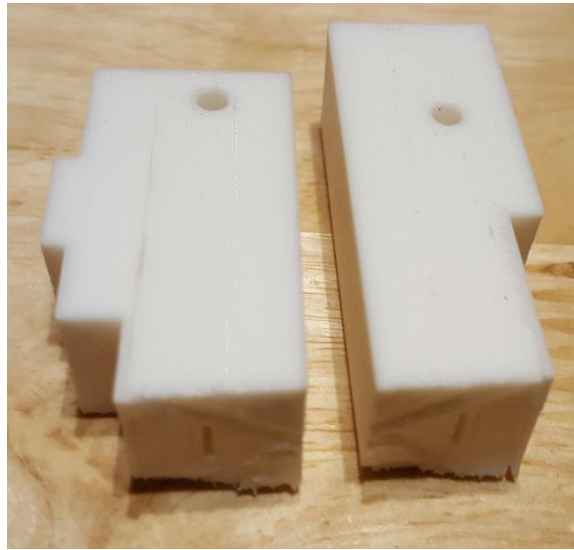


Figure A.3. Test Pump 1 view of cut microchannel



Figure A.4. Test Pump 1 print of cross section

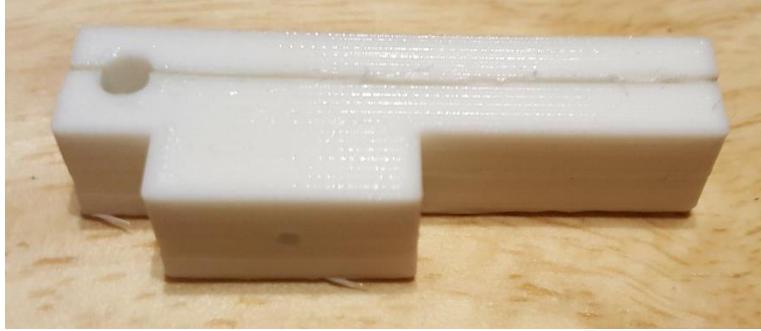


Figure A.5. Test Pump 2 (cut in half to investigate problems)

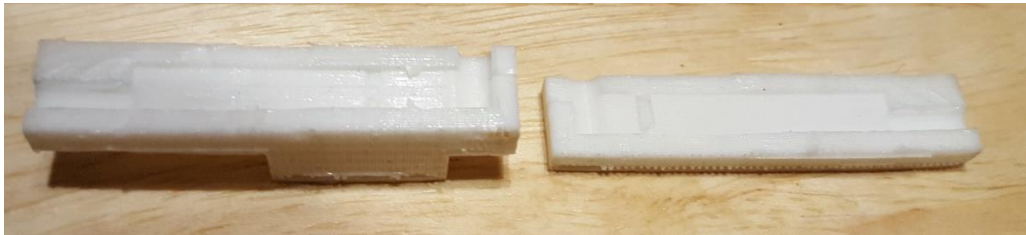


Figure A.6. Test Pump 2 cross section after cut

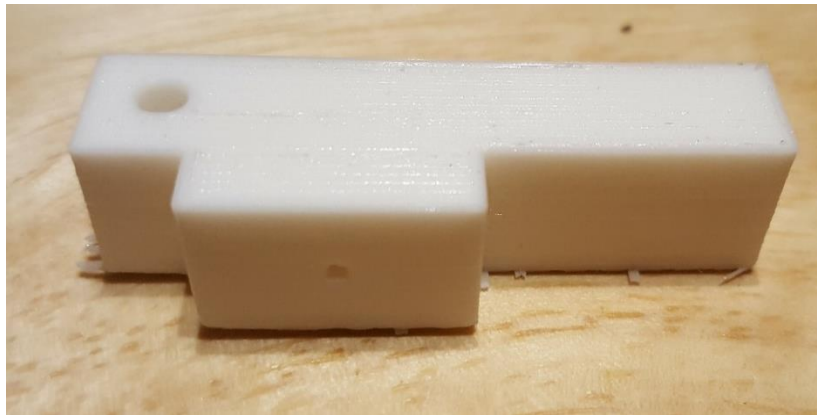


Figure A.7. Test Pump 3 (working micropump)



Figure A.8. Test Pump 4

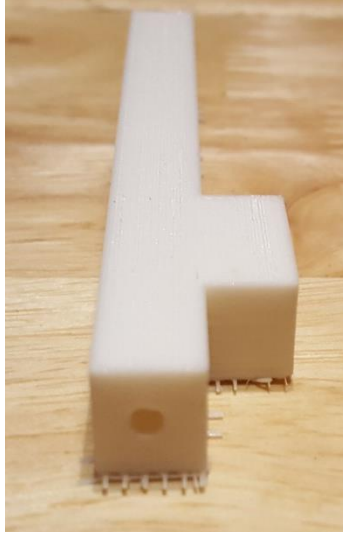


Figure A.9. Test Pump 4 with horizontal inlet

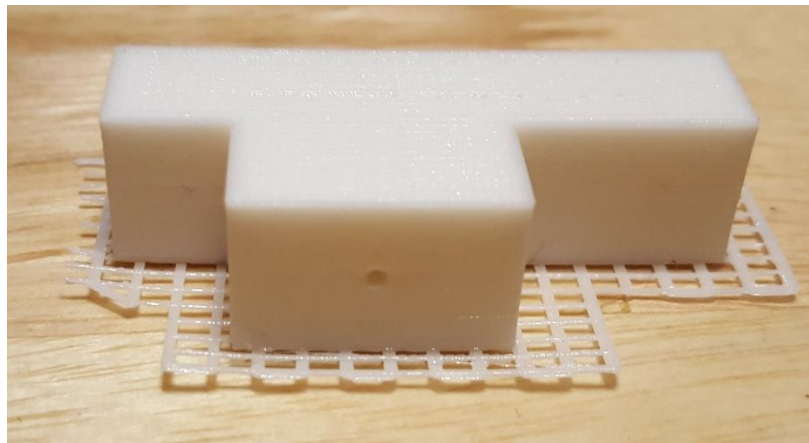


Figure A.10. Test Pump 5

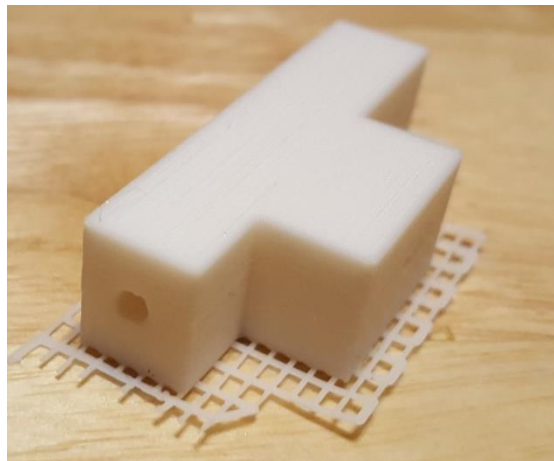


Figure A.11. Test Pump 5 with horizontal inlet